



Recent Progress in Model Development for the Time-Resolved Shielded Pickup Measurements of Electron Cloud Buildup

First models developed in 2010 (E-CLOUD10). Many modeling improvements since then:

- 1) Synrad3D photon rates and absorption site distributions*
- 2) Flexible photoelectron generation model (QE and energy distribution)*
- 3) More sophisticated, tuned SPU acceptance functions and hole secondary generation*
- 4) More accurate CESR vacuum chamber profile including vertical side walls*

Preparation for upcoming SPU data-taking with new unconditioned bare and TiN-coated aluminum v.c. at 15E/W.

Jim Crittenden & John Sikora

Cornell Laboratory for Accelerator-Based Sciences and Education

CESRTA Collaboration Meeting

21 August 2012



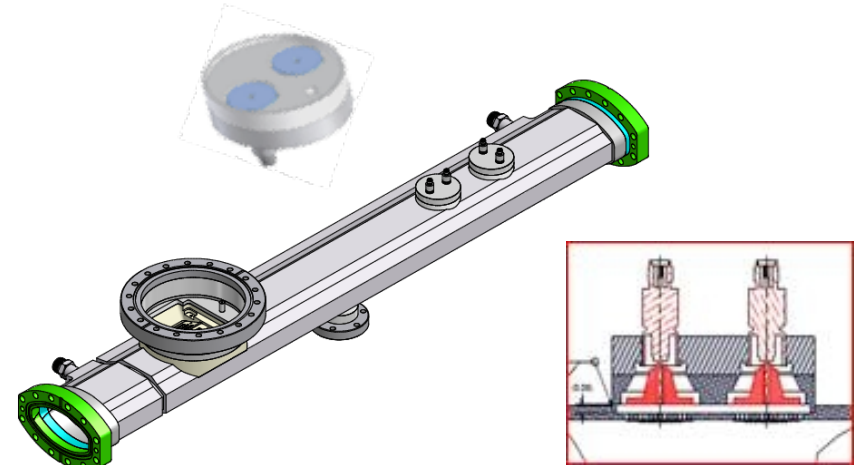
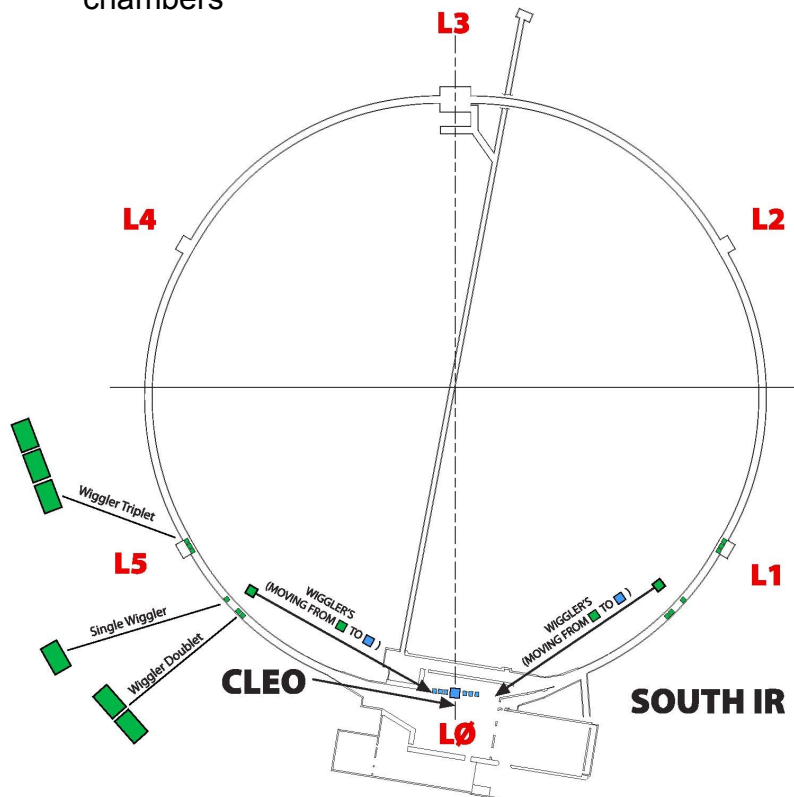


L3 Electron cloud experimental region

PEP-II EC Hardware:
Chicane, SEY station
Four time-resolved RFA's
Drift and quadrupole diagnostic chambers

New electron cloud experimental regions in arcs (after 6 wigglers moved to L0 straight)

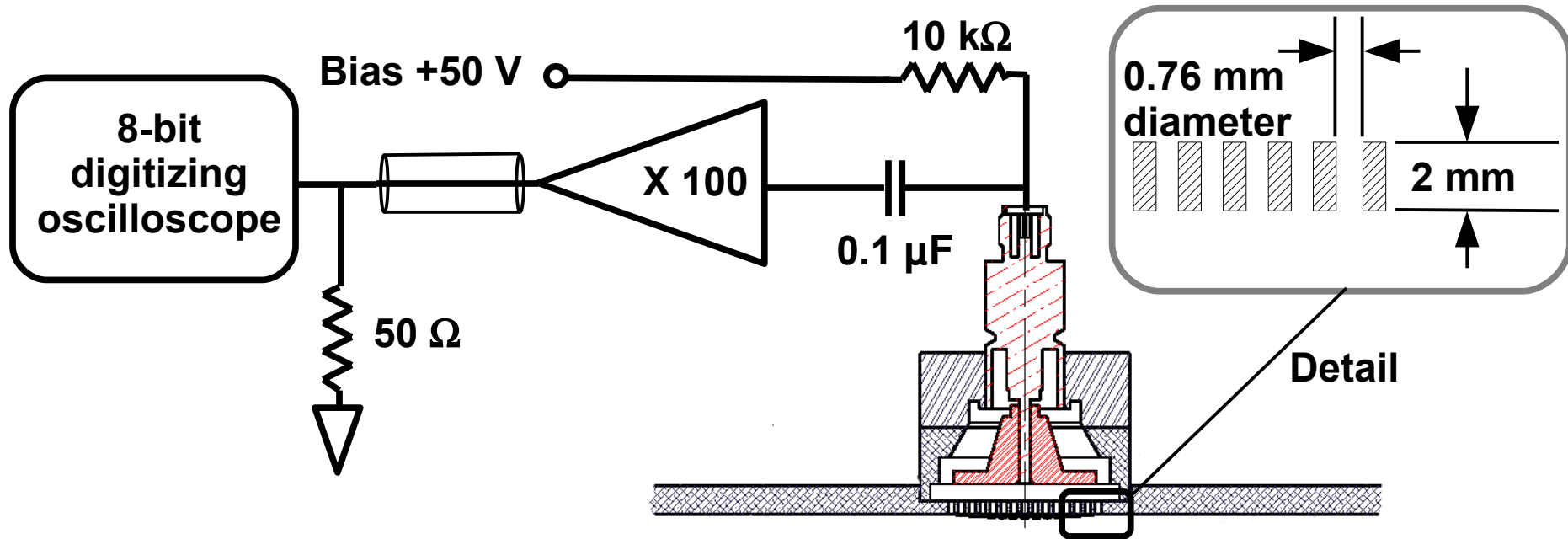
Locations for collaborator experimental vacuum chambers



Custom vacuum chambers with shielded pickup detectors

Uncoated aluminum, and TiN, amorphous carbon, diamond-like carbon coatings

30 RFA's in drift regions, dipoles, quadrupoles, and wigglers

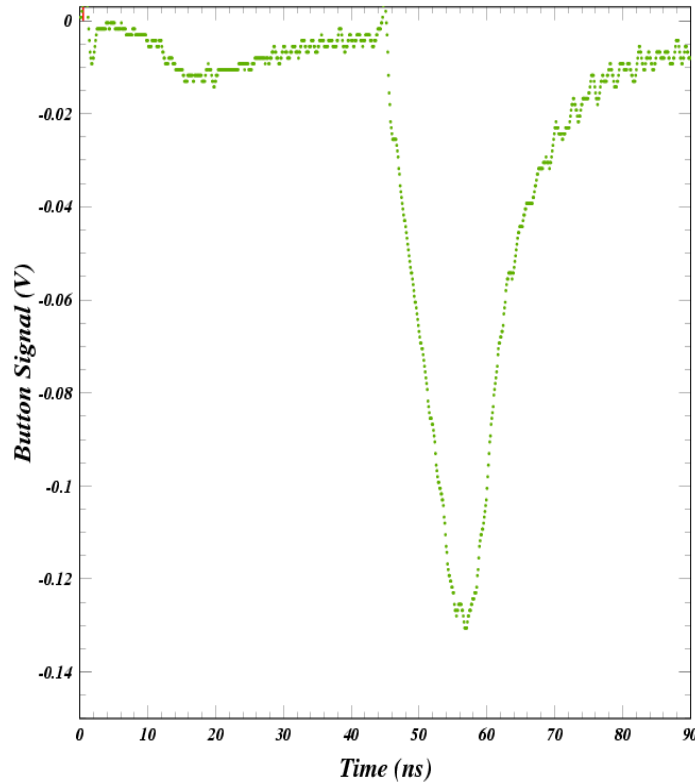


The pickup electrodes are shielded by the vacuum chamber hole pattern against the beam-induced signal.

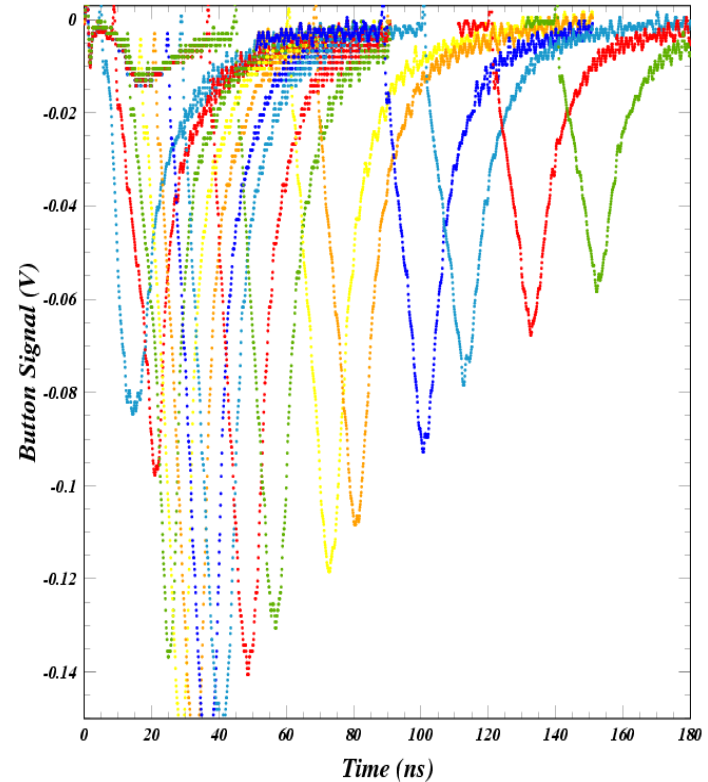
The positive bias ensures that secondaries produced on the electrode do not escape.



*Shielded pickup scope trace
for two bunches 44 ns apart*



*Superposition of 15 such traces
illustrating the sensitivity to cloud lifetime*



The single bunch signal arises from photoelectrons produced on the bottom of the vacuum chamber. Its shape is closely related to the photoelectron kinetic energy distribution and the beam kick. The witness bunch signal includes the single-bunch signal as well as the that produced by cloud particles accelerated into the shielded pickup by the kick from the witness bunch. The witness signal is therefore sensitive to SEY.



* Originated at CERN in the late 1990's

* Widespread application for PS, SPS, LHC, KEK, RHIC, ILC ...

* Under active development at Cornell since 2008

* Successful modeling of CESRTA tune shift measurements

* Interactive shielded pickup model implemented in 2010

* Full POSINST SEY functions added as option 2010-2012

* Flexible photoelectron energy distributions added 2011

* Synrad3D photon absorption distribution added 2011

I. Generation of photoelectrons

- A) Production energy, angle
- B) Azimuthal distribution (v.c. reflectivity)

II. Time-sliced cloud dynamics

- A) Cloud space charge force
- B) Beam kick
- C) Magnetic fields

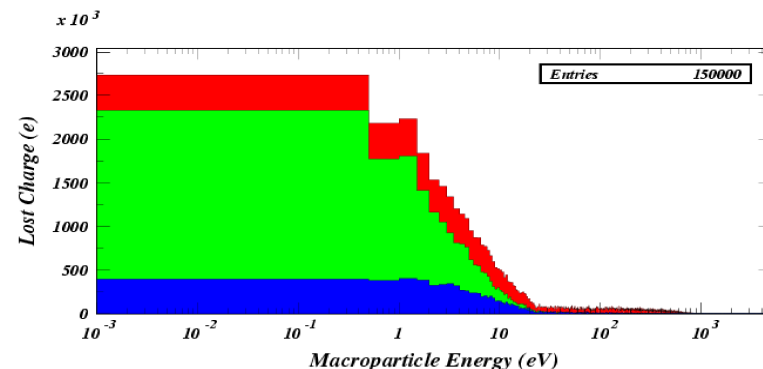
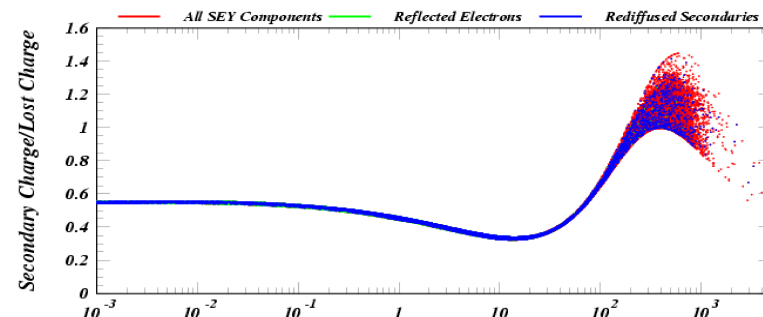
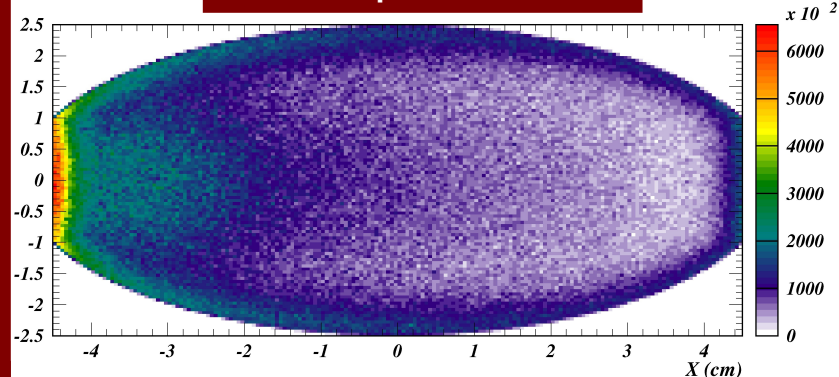
III. Secondary yield model

- A) True secondaries (yields > 1!)
- B) Rediffused secondaries (high energy)
- C) Elastic reflection (dominates at low energy)

IV. Shielded pickup model

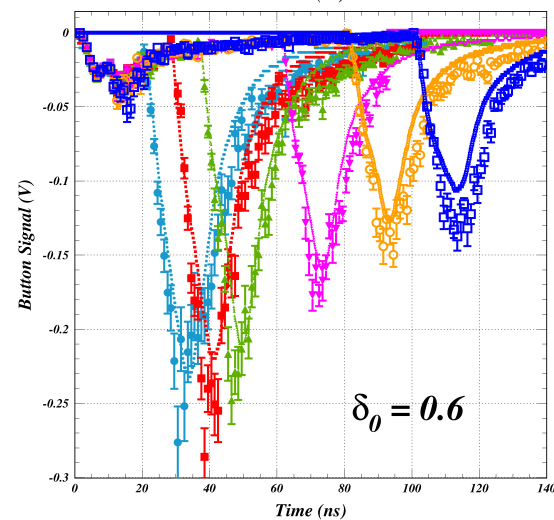
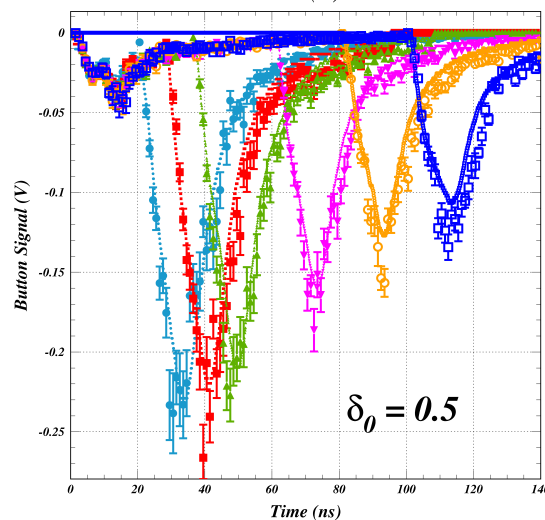
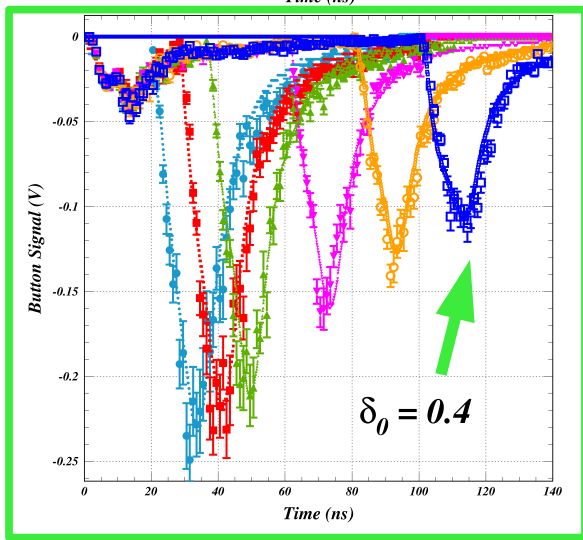
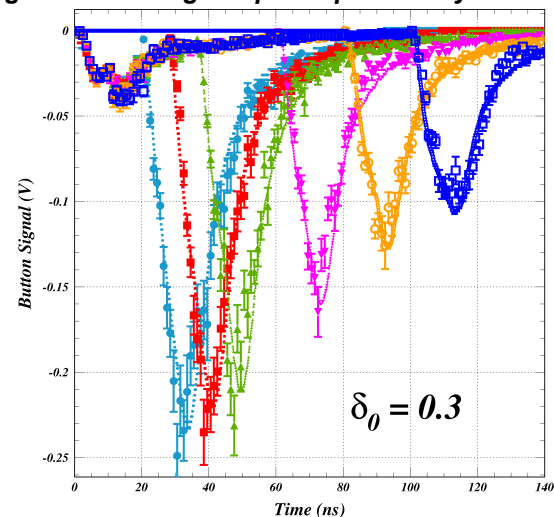
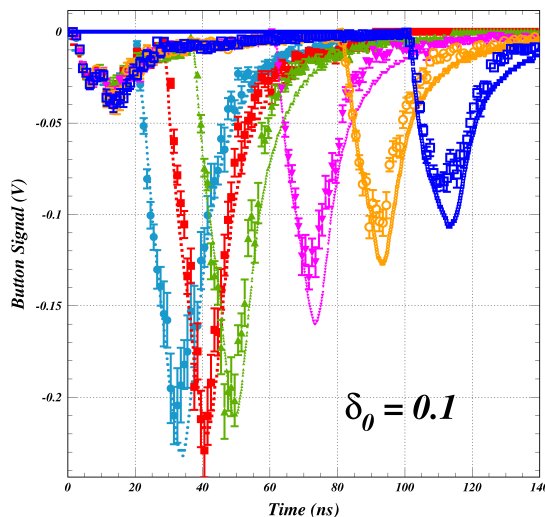
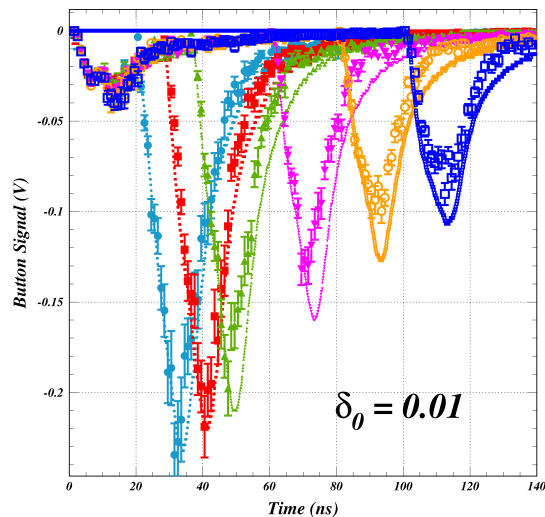
- A) Acceptance vs incident angle, energy
- B) Signal charge removed from cloud
- C) Non-signal charge creates secondaries

Cloud snapshot after 14 ns





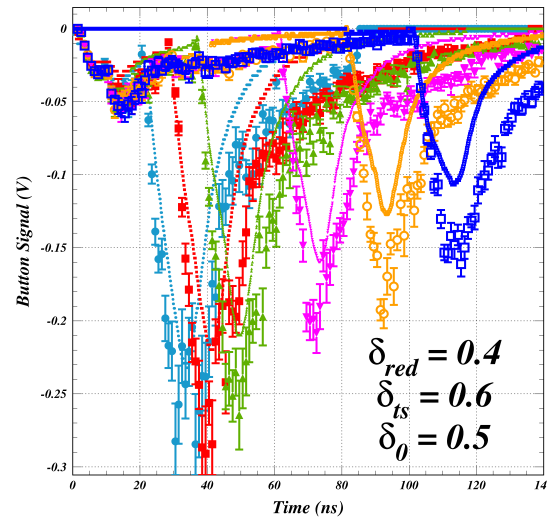
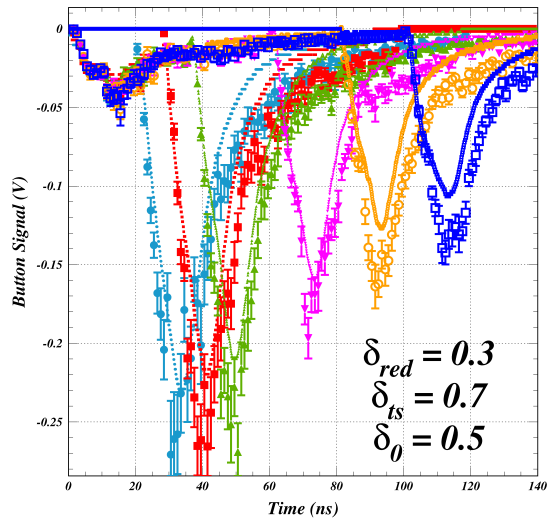
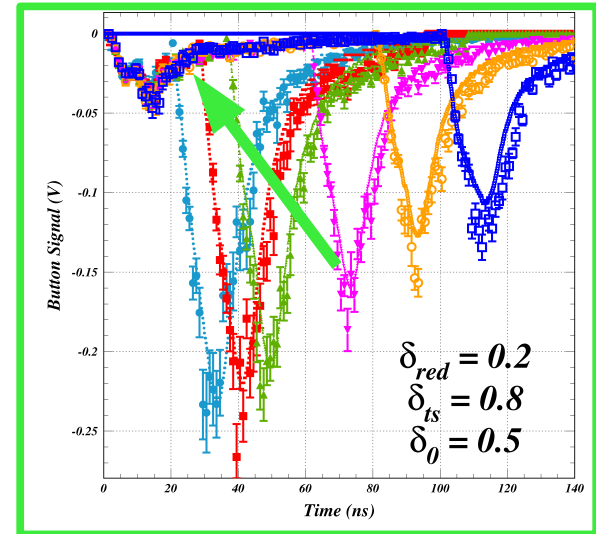
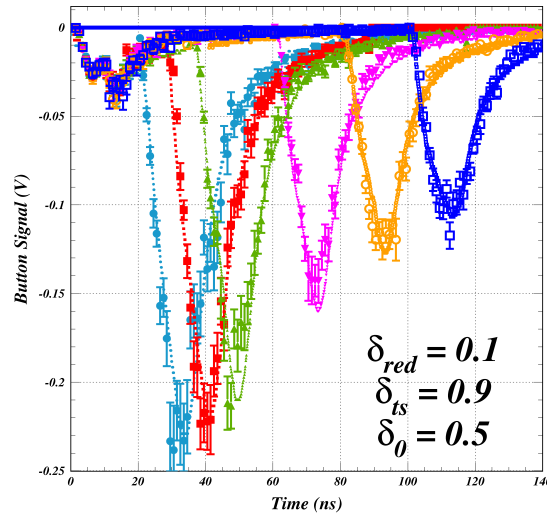
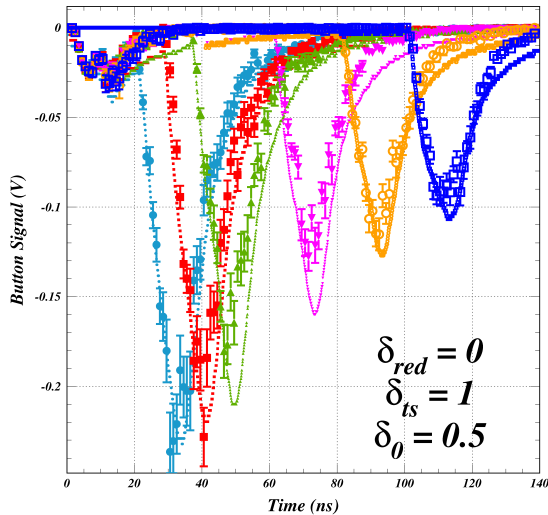
Work with NSF Research for Undergraduates Program participant Emily Hemingway



Satisfactory result after exhaustive parameter search (6 weeks!), but true secondary yield value LOW ($\delta_{ts} = 0.8$!)



Discriminating between the true and rediffused secondary yield processes



The rediffused secondary yield process determines the trailing edge of the signal from a single bunch.

This trailing edge is insensitive to δ_0 .

The late witness bunch signal used to determine δ_0 is also sensitive to the rediffused yield process.

The witness bunch method does provide discriminating power between the true and rediffused processes. But work remains to understand the low optimized value for the true secondary yield.



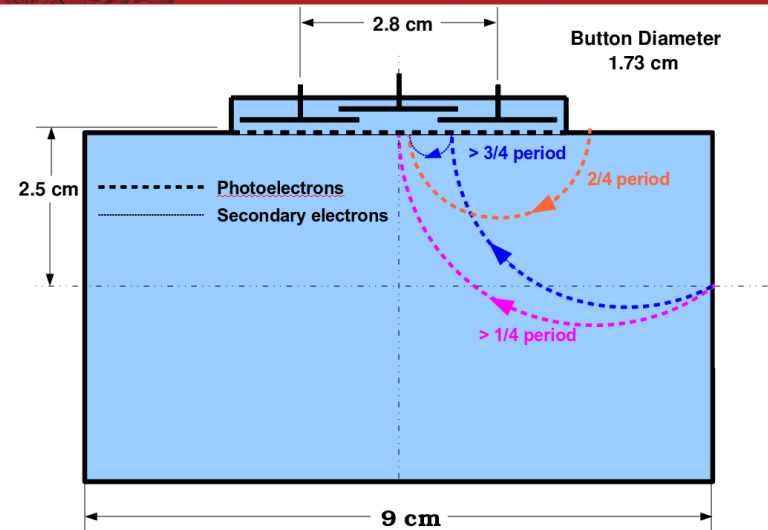
Understanding the SPU Signal Timing

The cyclotron motion of the photoelectrons determines when electrons sharing a production location contribute to the shielded pickup signal. The cyclotron period is

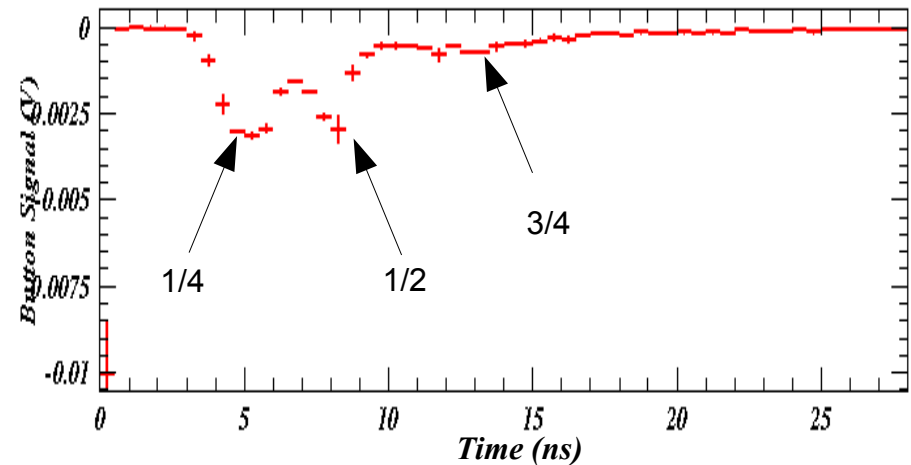
$$T = \frac{2\pi m}{qB}$$

The earliest signal corresponds to slightly more than one quarter period (>4 ns for a 23 Gauss field). A second pulse signal from photoelectrons produced on the ceiling arrives at about half a period. A third pulse from secondary electrons produced by photoelectrons on the ceiling arrives after about $\frac{3}{4}$ period. This late pulse is caused by photoelectrons that hit the ceiling, producing secondaries which curl up into the button after traveling an additional semi-circle.

The production location and angle of signal-producing photoelectrons depend on their kinetic energy, but the arrival times which determine the signal time structure depend only weakly on the energy.



ECLLOUD model of SPU signal development in a rectangular vacuum chamber
 $B=23$ G: $\frac{1}{4}$ period is 4 ns





Comparison of ECLLOUD model to observed signals for the case of the CESRTA vacuum chamber shape

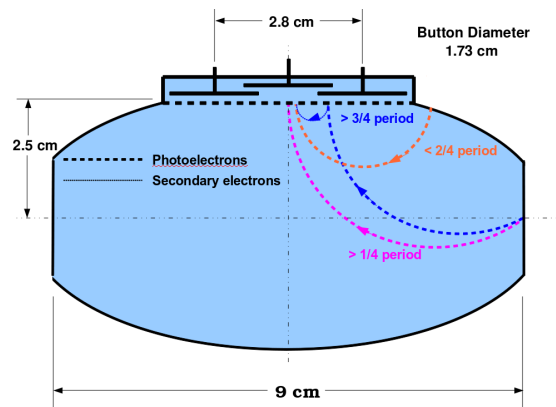
This comparison of modeled and measured SPU signals shows the effects of raising the modeled field strength to 12 G and 20 G in an ECLLOUD model which is a good match to the field-free case. This shows how the shape of the CESR beampipe affects the expected signal shape relative to the simple rectangular case.

The 20-G case (green) shows a double-pulse structure for the higher field which is not seen in the SPU signal. The two pulse times correspond approximately to $\frac{1}{4}$ cyclotron period for photoelectrons from the primary source point and $\frac{3}{4}$ cyclotron period for secondaries arriving after a single collision with the wall.

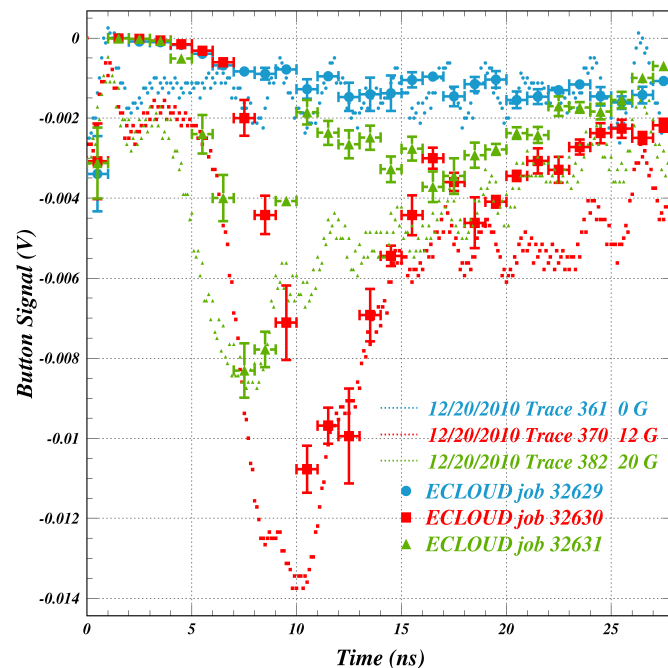
NB: One quarter cyclotron period ($T=2\pi m/qB$) is 4.5 ns for 20 Gauss and 7.5 ns for 12 Gauss for the central button. For this button, the cyclotron radius for photoelectrons from the primary source point is about 3 cm. Photoelectrons of energy near ~ 200 eV (125 eV) reach the central button for a field of 20 (12) Gauss.

The naïve extrapolation of the ECLLOUD model to nonzero solenoidal field results in a signal which arrives later than the measured one. Since the width of the button is in the simulation, this example shows that the button width does not suffice to explain the early signal.

Another candidate reason for early arrival times is the photoelectron production angular distribution, which can produce path lengths shorter than a quarter cyclotron period.

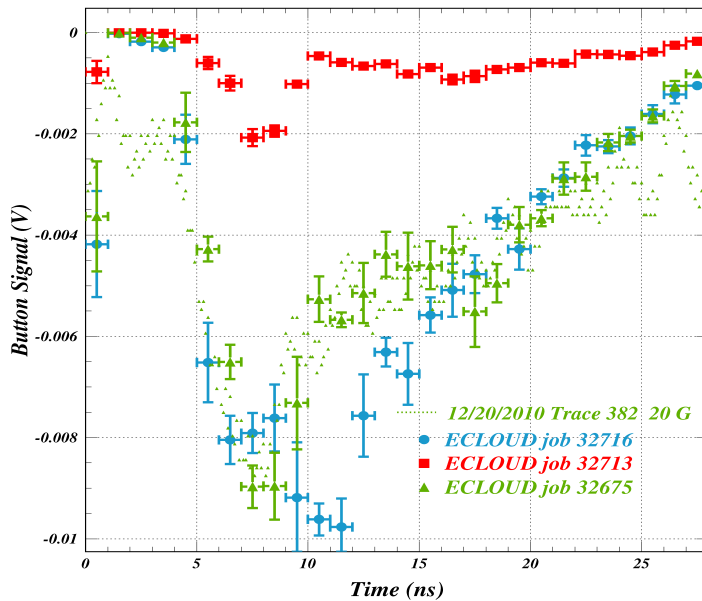


Solenoid scan: 2.085 GeV 4.1 mA/bunch e- 15E a-C





Solenoid scan: 2.085 GeV 3.8 mA/bunch e- 15E a-C



The energy distribution for photoelectrons produced by s.r. photons absorbed at the primary source point used up until this point corresponds to the red points. We now add a higher-energy component with a weight of 75%.

Two Power-Law Contributions

$$F(E) = E^{P_1} / (1 + E/E_0)^{P_2}$$

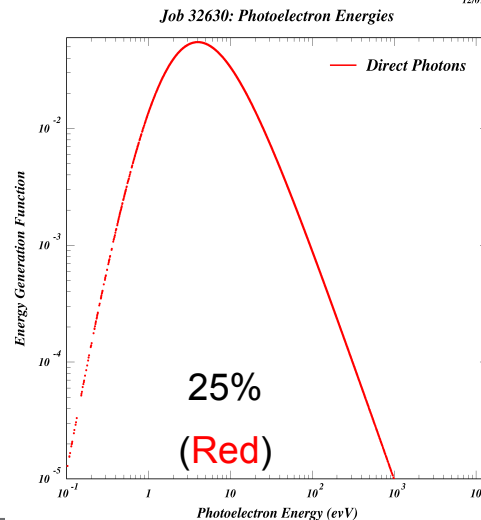
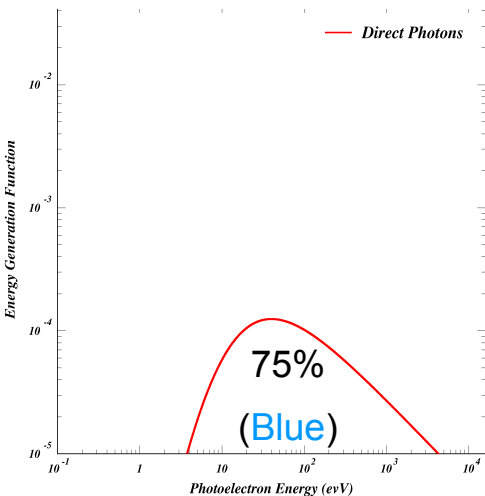
$$E_0 = E_{peak} (P_2 - P_1) / P_1$$

$$E_{peak} = 40 \text{ eV} \quad P_1 = 4 \quad P_2 = 4.7$$

The high-energy component (75%) has a peak energy of 40 eV and an asymptotically falling power of 0.7. Its contribution to the signal is shown in light blue.

$$E_{peak} = 4 \text{ eV} \quad P_1 = 4 \quad P_2 = 6$$

The low-energy component (25%) has a peak energy of 4 eV and an asymptotically falling power of 2. Its contribution to the signal is shown in red.



12/07/20 12:09



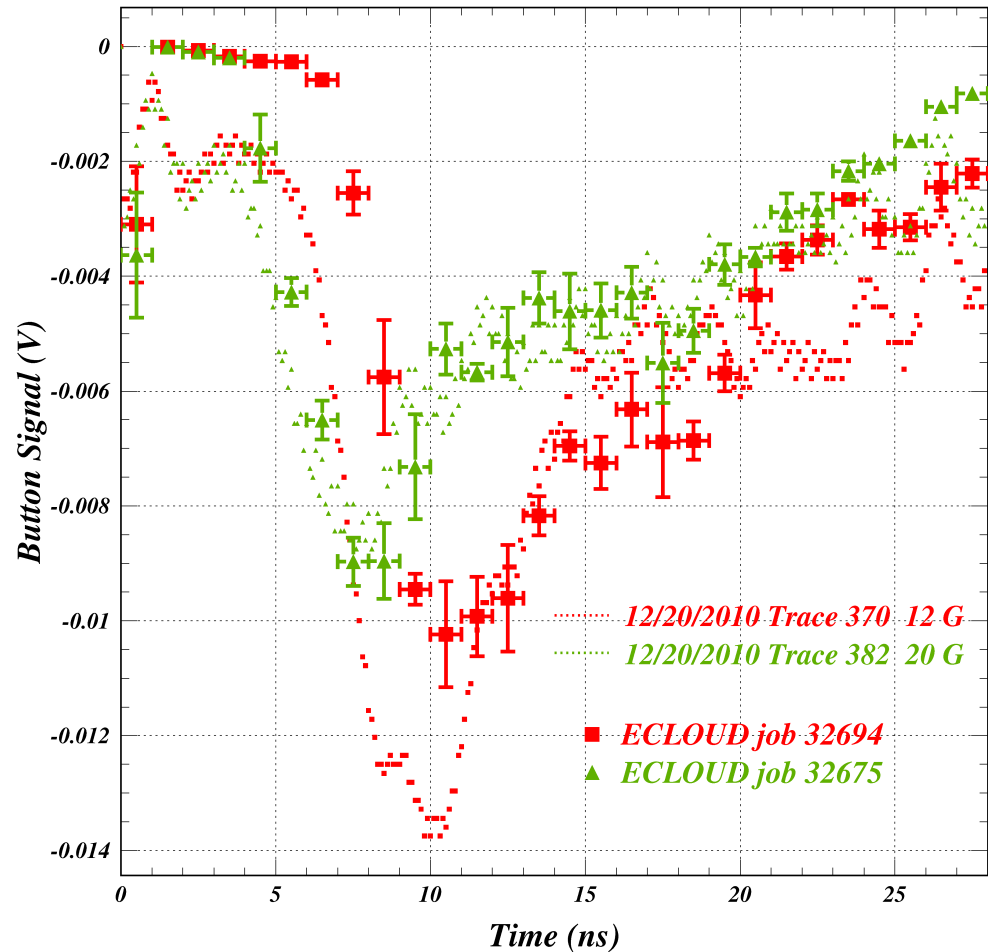
Comparison of 20 Gauss and 12 Gauss simulations

Here are the 20G (green) and 12G (red) simulations side by side.

The modeled signal for 12 G is smaller than measured. The model which correctly produces the leading edge timing for 20 G produces a signal for 12 G which is late. Note, that given the difference in cyclotron periods for 12 G and 20 G fields ($7.5 \text{ ns} - 4.5 \text{ ns} = 3.0 \text{ ns}$) the rising edge of the simulation shows the expected time shift of 3 ns, whereas the data show only a 2 ns separation.

The comparison of the observed signal time shift to the ECLLOUD modeling results indicates that the change in field magnitude is much less than expected from the power supply current settings, i.e. closer to 2 G than 8 G.

Solenoid scan: 2.085 GeV 3.8 mA/bunch e^- 15E a-C





This Summer's Progress in Modeling Electron Cloud Buildup in Solenoidal Magnetic Fields Using Shielded Pickup Measurements

- **Understanding of the time structure of the SPU signal in a solenoidal field**
 - The basic structure of the pulse is determined by the cyclotron period. Changing from a rectangular pipe to one with a more rounded shape smears out the signal, but in an understandable way.
 - The observation of cloud electrons which contribute to a signal prior to the quarter cyclotron period motivated study of their possible origin. The p.e. production angular distribution was removed as a possible answer. An in-depth study of the relationship between p.e. production energy and signal arrival time succeeded in modeling the early signal via the introduction of a second power-law contribution.
- **Identifying issues in the field strength dependence of the model**
 - Changing the modeled magnetic field strength raises further issues. The simulation matches the expected time shift well, but the observed signal does not. This may be due to an error in the assumed solenoid excitation calibration. But it may also be that the expectation for the time shift is too naïve, owing to the complicated influence of the photoelectron energy distribution. Only a full model can resolve this issue.
- **Next steps**
 - Investigate further optimization of model parameters
 - New measurements with Helmholtz coils having replaced simple wire windings at 15E/W.

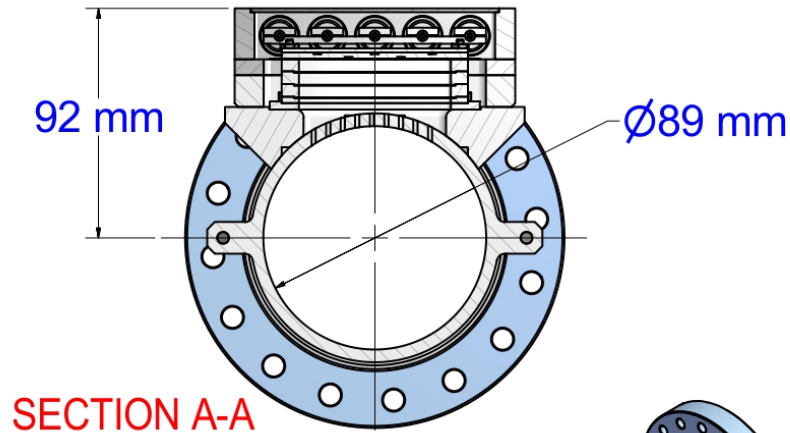


- *Continue work on the present model for uncoated aluminum.*
 - ➔ *Why is the optimized peak yield value so low?*
 - ➔ *It is a poor match to the data for bunch spacings less than 20 ns. Why?*
- *Develop the model for the TiN-coated vacuum chamber at 15W.*
 - ➔ *SPU measurements in a conditioned TiN-coated chamber at 15W were made 12/2010, 4/2012, 6/2012.*
- *Take full set of witness bunch measurements on new Al and TiN: 22-23 August.*
 - ➔ *Immediate comparison to the model to see if SEY yields are indeed higher.*
 - ➔ *Repeat in November to see conditioning effects.*
- *Develop a model for the time-resolved RFA detectors in L3.*
 - ➔ *SPU acceptance functions and collector definitions needed.*

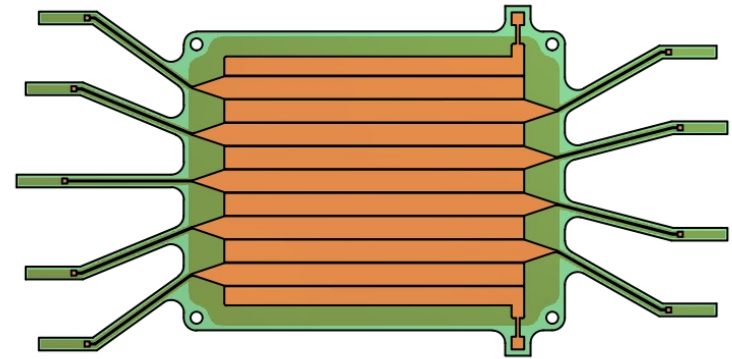


New Time-Resolved RFA's in L3

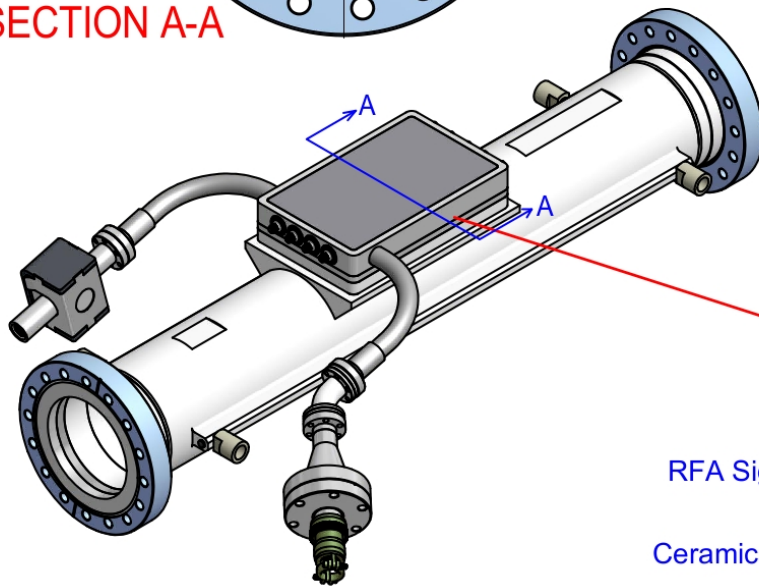
Four v.c.: bare and TiN-coated Al, both smooth and grooved



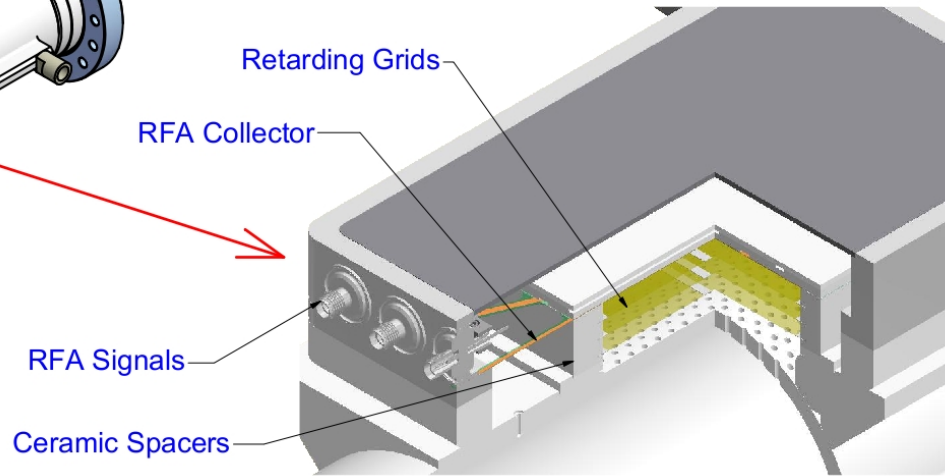
SECTION A-A



RFA Collector with 9 channels



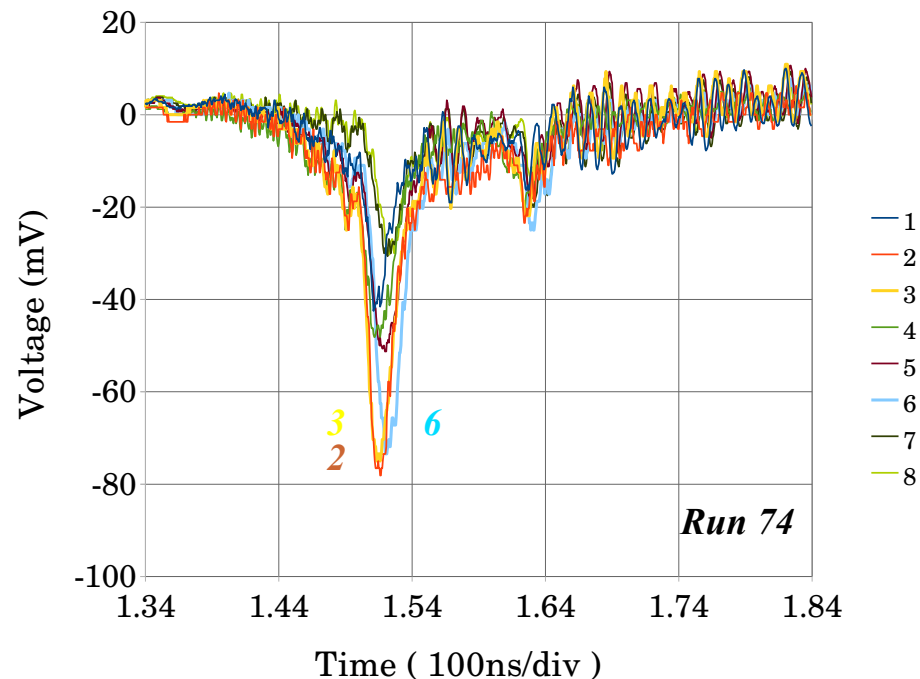
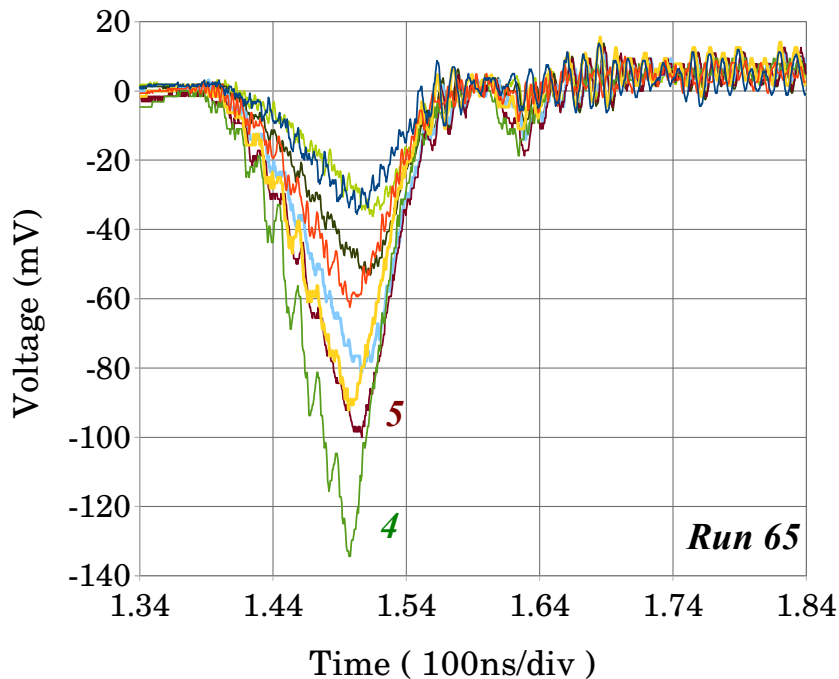
TR-RFA Vacuum Chamber



RFA Structure Detail



3/13/2012 5.3 GeV e+ 10 bunches 8 mA/bunch Al (L3#4)



Chicane dipole field off

Central collectors dominate.

Chicane dipole field 45 G

Central collectors show a depletion zone.
This is known to arise from the peak of the SEY curve and provides information on E_{\max} .